$$\text{"}C_1\text{"} \quad \text{for} \quad \frac{T_1 C\pi^3}{4g}\sqrt{\frac{\pi}{2}} \tag{28}$$

and:

$$\text{"}C_2\text{"} \quad \text{for} \quad \frac{3}{32}\frac{\rho C\pi^3}{g^2}\sqrt{\frac{\pi}{2}} \quad . \tag{29}$$

It turns out that, on using $T_1 = 74$ dynes/cm,

$$\begin{aligned} C_1 &= 6.1 \times 10^{-4} \text{ dyne cm}^{-2} \text{ sec} \\ C_2 &= 3.2 \times 10^{-9} \text{ gm cm}^{-5} \text{ sec}^3 \quad . \end{aligned} \tag{30}$$

In the cgs system, so that U_a is in centimeters per second and $\mathcal{E}$ in ergs per centimeter squared.

From (27) we can see that for small winds, i.e., $U_a << 1$ (in whatever units) the linear power of U_a will be *relatively* dominant, so that capillary waves will contribute most of the energy $\mathcal{E}$. For greater winds, i.e., $U_a >> 1$, the fifth power of U_a takes dominance, and gravity waves will hold the lion's share of energy. In this way we have made quantitative the intuition we already possessed about the energy $\mathcal{E}$ in our discussions of (98) of Sec. 12.3.

12.9 Theoretical Wave Spectra Models

In this section we shall review some of the empirical data and models discussed in Secs. 12.5-12.8 from a relatively theoretical vantage point with the purpose in mind of "rationalizing" the empirical results and embedding them in a plausible conceptual framework. In particular, we shall show how one can view the gaussian frequency distributions of wave elevations and slopes as the result of the steady confluence of great numbers of independent simple wave events. Some of the wave spectra of Sec. 12.8 can also be viewed in this way. However, a matter which cannot yet be so simply viewed is the *generation process* of the wave spectra. The mathematical description of this process is still incomplete. Some current approaches to this description problem will be outlined in the closing paragraphs of this section.

The Wave Elevation Distribution

Experimental evidence for the gaussian form of the distribution of wave crest elevations about a mean sea level under open sea, steady state wind conditions is now largely established (cf., e.g., Fig. 12.46). We can construct a simple mathematical basis for this empirical fact as follows. Imagine a uniformly graduated vertical pole fixed into the sea bottom and visualize the wave profile moving up and down along the pole as the waves go by (Fig. 12.53). Suppose that

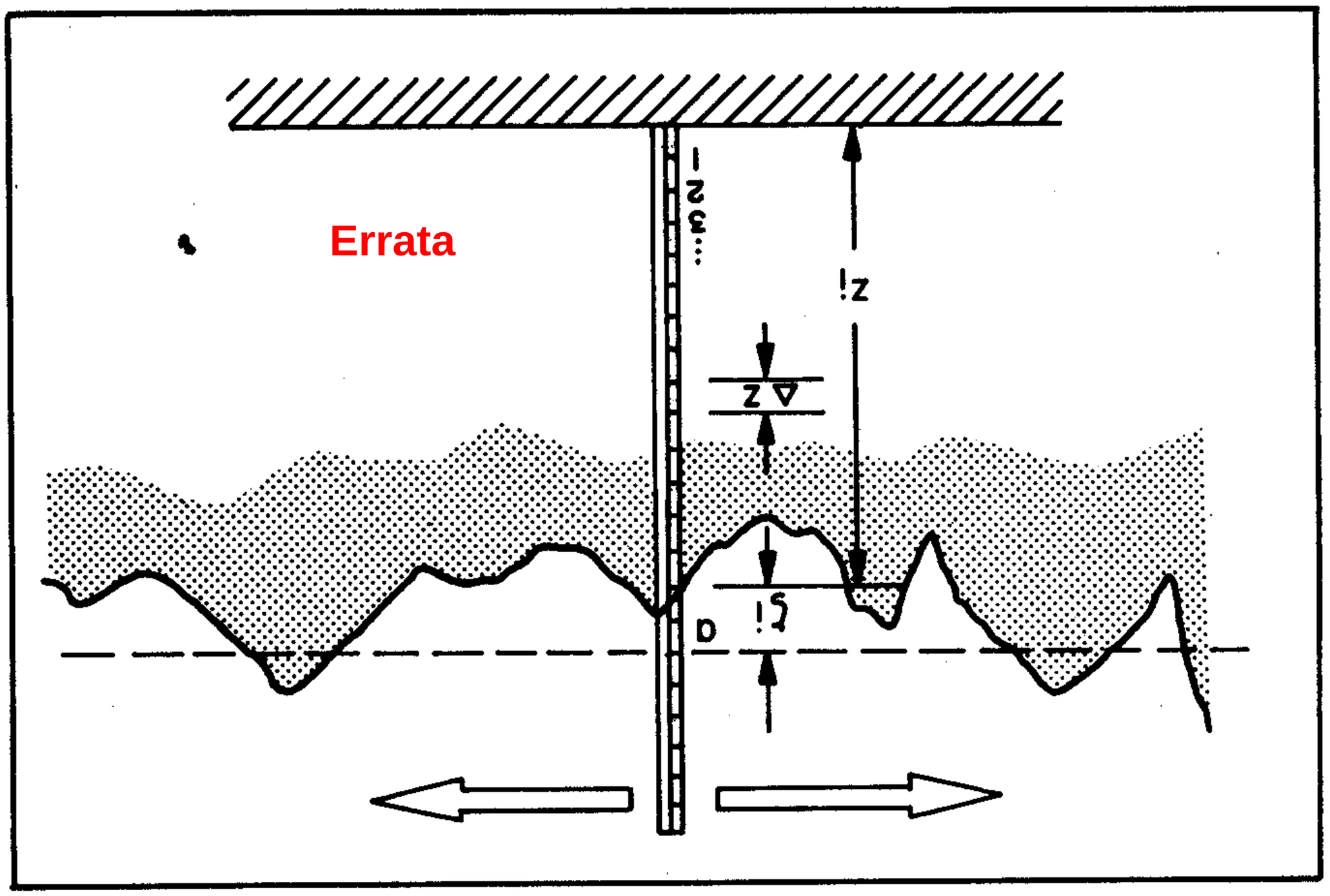

FIG. 12.53 Setting for a theoretical derivation of the wave-elevation distribution and its close relatives.

an arbitrary large number $z_1, z_2, \ldots, z_n$, of depth readings along the pole are taken, and let $\phi_1(z_i)$ be the relative number of times the depth occurred in the small Δz interval about depth z_i. ϕ_1 then is an empirically determined probability function. For a large number n of readings spaced reasonably far apart in time, our intuition tells us that a histogram of $\phi_1(z_i)$ versus z_i would cluster around some mean depth, say a, *and fall off on either side of depth a.* Hence ϕ_1 attains a maximum value at a. Even though we do not know the form of ϕ_1, at least that much should be granted, and granting this is the first crucial step in the derivation.

The next thing we do is compute the mean elevation a from the sample z_i, i = 1, 2, ..., n:

$$a = \frac{1}{n}(z_1 + z_2 + \ldots + z_n) \qquad (1)$$

Then we agree to refer all elevations to a, so that if ζ_i is any observed elevation, we write:

$$\text{"}\zeta_i\text{"} \quad \text{for} \quad z_i - a$$

and

$$\text{"}\phi(\zeta_i)\text{"} \quad \text{for} \quad \phi_1(z_i) \qquad (2)$$

Now using ϕ, we compute the probability $P_n(\zeta_1, \zeta_2, \ldots, \zeta_n)$

that any arbitrary given set $\zeta_1, \zeta_2, \ldots, \zeta_n$ of elevations about the mean level a will occur. The second crucial step in the present derivation is the assumption that *these n elevations are statistically independent*, so that

$$P_n(\zeta_1, \zeta_2, \ldots, \zeta_n) = \phi(\zeta_1)\phi(\zeta_2) \ldots \phi(\zeta_n) \quad . \qquad (3)$$

Now for our present purposes, P_n can be thought of as a function of a single variable, namely the mean depth a, with the z_i being arbitrary and fixed throughout the discussion. Since the samples $z_1, z_2, \ldots z_n$ are depths drawn from a population whose mean is (estimated by) the depth a, it is at least intuitively clear that, since ϕ has a maximum at $\zeta = 0$, $P_n(\zeta_1, \zeta_2, \ldots, \zeta_n)$ should have a maximum when the variable a takes on the true values of the population mean of $z_1, z_1, \ldots, z_n$ (this is a maximum likelihood argument; see for example [59]). Hence we set

$$\frac{dP_n}{da} = 0 \quad . \qquad (4)$$

Using the representation (3) of P_n, the condition (4) yields

$$\phi'(\zeta_1)\phi(\zeta_2)\ldots\phi(\zeta_n)\frac{d\zeta_1}{da} + \phi(\zeta_1)\phi'(\zeta_2)\ldots\phi(\zeta_n)\frac{d\zeta_2}{da} + \ldots$$

$$+ \phi(\zeta_1)\phi(\zeta_2)\ldots\phi'(\zeta_n)\frac{d\zeta_n}{da} = 0 \qquad (5)$$

where the prime denotes differentiation of ϕ with respect to its argument ζ. From (2) we have

$$\frac{d\zeta_i}{da} = -1$$

for each i = 1, 2, ..., n; so that (5) can be reduced to

$$\frac{\phi'(\zeta_1)}{\phi(\zeta_1)} + \frac{\phi'(\zeta_2)}{\phi(\zeta_2)} + \ldots + \frac{\phi'(\zeta_n)}{\phi(\zeta_n)} = 0 \quad . \qquad (7)$$

By (1) and (2):

$$\mu(\xi_1 + \xi_2 + \ldots + \xi_n) = 0 \quad , \qquad (8)$$

for any constant μ. Subtracting (8) from (7), term by term:

$$\left(\frac{\phi'(\zeta_1)}{\phi(\zeta_1)} - \mu\zeta_1\right) + \left(\frac{\phi'(\zeta_2)}{\phi(\zeta_2)} - \mu\zeta_2\right) + \ldots + \left(\frac{\phi'(\zeta_n)}{\phi\ \zeta_n)} - \mu\zeta_n\right) = 0 \qquad (9)$$

Since our choice of the z_i (and hence the ζ_i) was arbitrary, we have:

$$\frac{\phi'(\zeta_i)}{\phi(\zeta_i)} - \mu\zeta_i = 0 \qquad (10)$$

for every i, which is a simple differential equation in ϕ, the general solution of which is:

$$\phi(\zeta) = Ae^{\mu\zeta^2/2} \quad . \qquad (11)$$

The requirement that ϕ have a maximum at $\zeta = 0$ requires μ be negative. Therefore, $\mu = -1/m$ for some positive number m so that (11) can be written:

$$\boxed{\phi(\zeta) = Ae^{-\zeta^2/2m}} \quad . \qquad (12)$$

It turns out that $A = 1/\sqrt{2\pi m}$ under the requirement that:

$$\int_{-\infty}^{\infty} \phi(\zeta)d\zeta = 1 \quad . \qquad (13)$$

Errata By a straightforward computation, it is clear that m is simply the mean square deviation m of the elevation from the mean elevation discussed all during this chapter (cf. (89) of Sec. 12.3). In this way, assuming only the independence of wave elevations in an arbitrary sequence of recordings, and that the mean wave elevation occurs most often of all elevations, we arrive at the gaussian frequency distribution of wave elevations. Of course there are several fine points on the differentiability of the empirical function ϕ and the continuity of its variables ζ that would be more fully discussed in a rigorous derivation. However, even then, the essential two properties leading to (12) will be those enunciated above.

The Wave Slope Distribution

Experimental evidence that the form of the distribution of wave slopes about the zero mean slope is, to a first approximation, a gaussian distribution, may now be considered well established, principally through the work of Duntley (cf. (13) of Sec. 12.5) and Cox and Munk (cf. (26) of Sec. 12.5). Our present aim is to deduce this observed slope distribution from a small set of physically plausible assumptions; in this way we may explain its observed form.

In order to lend a semblance of concreteness to the derivation, we shall adopt the Duntley sea state meter (Sec. 12.5) as the instrument yielding the various hypothetical readings used in the derivation. Thus imagine that the slope readings are processed and reduced to pairs (ξ_1,η_1), (ξ_2,η_2), ..., $(\xi_n,\eta n)$ where ξ_i is the ith up-down wind slope

reading and η_i the corresponding cross-wind slope reading taken at the same time, and normalized using (24) and (25) of Sec. 12.5. We use the wind reference frame for concreteness. There is no essential modification of the derivation if a terrestrial or sun-based reference frame is adopted. If these pairs of readings are plotted in a $\xi\eta$ coordinate system, a scattering of points, such as those schematically appearing in part (a) of Fig. 12.54, is obtained. By using ξ and η, the *scatter diagram is* found to be basically *symmetric about the origin and decreases in density in all directions away from the origin.* We shall adopt this property as an initial assumption. If we had used a different reference frame obtained by rotating the $\xi\eta$ frame through an angle θ, the inherent circular form of the distribution, of course, would not change, only the coordinates of its individual

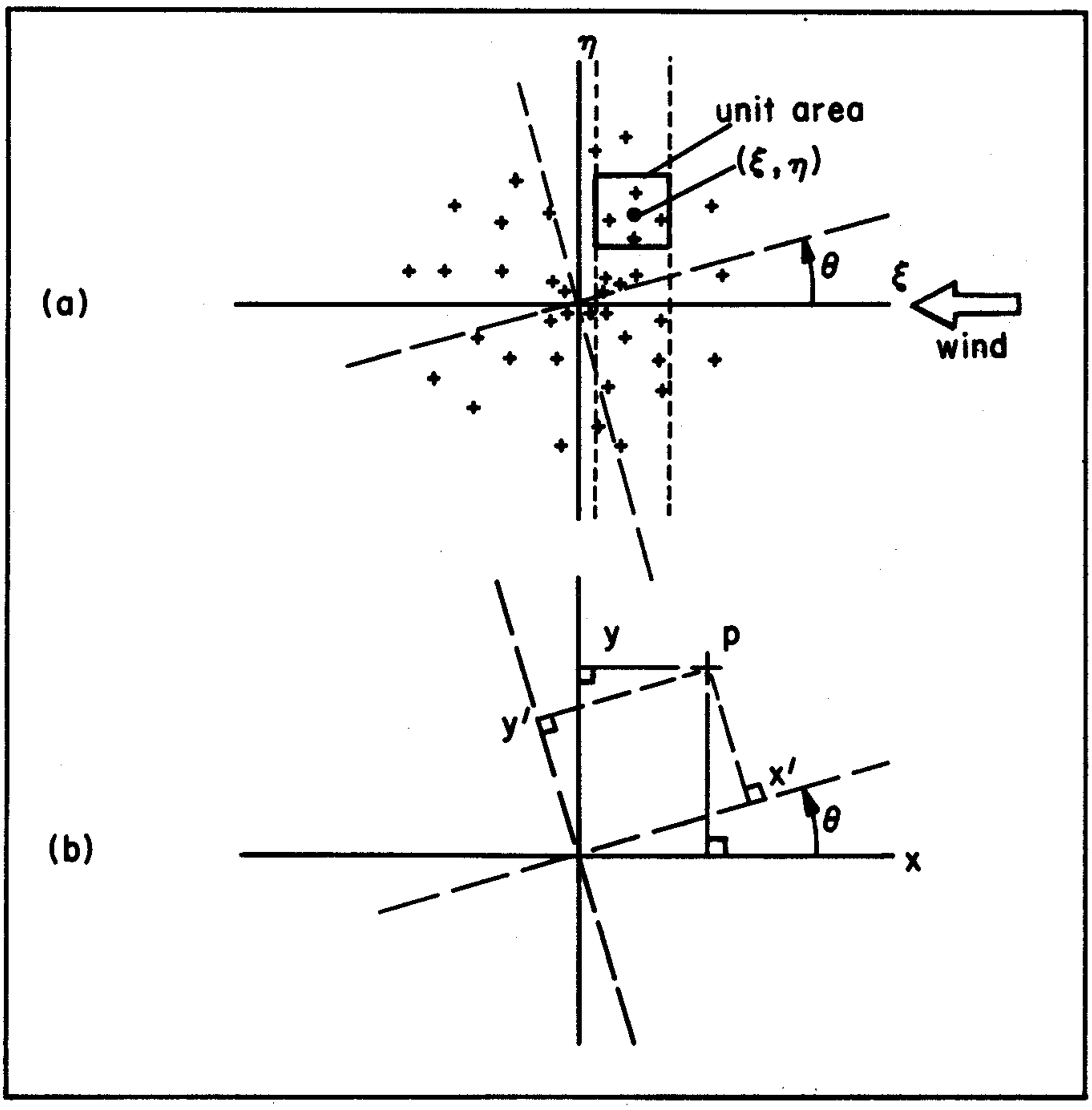

FIG. 12.54 Setting for a theoretical derivation of the wave-slope distribution.

points would change. Furthermore, the distance of (ξ,η) from the origin would not change during a rotation of coordinates. This is clear geometrically from Fig. 12.54, but actually can be verified from simple transformation equations. Since this fact plays an important role in the derivation, we will now indicate its proof, since not all physical quantities are invariant under such changes of coordinate systems. For example, if we had adopted the concept of the inclination of the surface; that is, *angles* rather than *tangents of angles*, then the present derivation would not go through as naturally; in this way we see the judiciousness of the choice of wave *slopes* rather than wave *inclincations*, by the original experimenters, as the appropriate variables which are distributed in a gaussian manner.

A rotation of coordinates of the sea surface through an angle θ is depicted in (b) of Fig. 12.54. The new coordinates (x',y') of point P relative to the x'y' frame are related to the coordinates of P in the xy frame by (the geometrical details in Fig. 12.22 may be used here also):

$$\begin{aligned} x' &= x \cos\theta + y \sin\theta \\ y' &= -x\cos\theta + y\cos\theta \quad , \end{aligned} \tag{14}$$

and conversely:

$$\begin{aligned} x &= x' \cos\theta - y' \sin\theta \\ y &= x' \sin\theta + y' \cos\theta \ . \end{aligned} \tag{15}$$

If the orientation of the air-water surface is given by (ζ_x,ζ_y) in the original frame, then in the new frame we have, by the chain rule for partial differentiation:

$$\zeta_{x'} = \zeta_x \frac{\partial x}{\partial x'} + \zeta_y \frac{\partial y}{\partial x'} = \zeta_x \cos\theta + \zeta_y \sin\theta$$

$$\zeta_{y'} = \zeta_x \frac{\partial x}{\partial y'} + \zeta_y \frac{\partial y}{\partial y'} = -\zeta_x \sin\theta + \zeta_y \cos\theta \quad .$$

From these representations, we see that

$$\zeta_{x'}^2 + \zeta_{y'}^2 = \zeta_x^2 + \zeta_y^2 \quad .$$

This result is a purely geometric property of slopes. Similarly, by now going over into the (ξ,η) coordinate system, in which the distribution is centrally symmetric about the origin, it follows from (12) or (15) that:

$$(\xi')^2 + (\eta')^2 = \xi^2 + \eta^2 \quad , \tag{16}$$

as was to be shown. The stablishment of (16) constitutes the first step of the derivation.

The second step of the derivation adopts the second and final assumption; namely, that of the *statistical*

Errata

independence of the wave slope components ξ and η. The analytic form this assumption takes is obtained as follows. Suppose that $\Phi(\xi,\eta)$ gives the fractional number of crosses per unit area (in slope space) at (ξ,η) in the scatter diagram (a) of Fig. 12.54. Experimental evidence indicates that there is some frequency function ϕ such that:

$$\Phi(\xi,\eta) = \phi(\xi)\phi(\eta) \quad , \tag{17}$$

and by the circular symmetry of the scatter diagram (a) of Fig. 12.54, this ϕ is independent of θ. In other words, if we took vertical slices (i.e., with ξ fixed) of the scatter diagram, as shown in (a) of Fig. 12.54, and the relative frequency of crosses in that slice is found as a function of η, then the functional *form of that frequency function* is to be independent of ξ. In a similar way we could consider horizontal slices of constant η. This property of ϕ would, then, be independent of the orientation θ of the coordinate frame relative to the wind-based frame. As noted above, we have essentially erased the assymetry of the wind in the slope distribution by adopting the normalized coordinates $\xi(= \zeta_x/\sigma_u)$ and $\eta(= \zeta_y/\sigma_c)$.

It follows from (16) and (17) that ϕ obeys the functional equation:

$$\phi(\xi)\phi(\eta) = \phi((\xi^2 + \eta^2)^{1/2})\phi(0) \quad . \tag{18}$$

This may be seen by representing $\Phi(\xi,\eta)$ in two successive ways by rotating the reference frame between two fixed orientations so that the ξ axis goes through the point (ξ,η). For the general prerotation case, we have:

$$\Phi(\xi,\eta) = \phi(\xi)\phi(\eta) \tag{19}$$

for the post rotation case we have

$$\Phi(\xi',\eta') = \phi(\xi')\phi(\eta') \tag{20}$$

where $\xi' = (\xi^2 + \eta^2)^{1/2}$, $\eta' = 0$.

By the circular symmetry of the scatter diagram in (a) of Fig. 12.54,

$$\Phi(\xi,\eta) = \Phi(\xi',\eta')$$

whenever ξ,η and ξ',η' are such that $\xi^2 + \eta^2 = (\xi')^2 + (\eta')^2$. This last condition is by (16) now the case, by virtue of rotation transformations of the kind (14) or (15). Equation (18) now follows from (19) and (20) and the preceding equation. The determination of the functional relation (18) for ϕ constitutes the third step of the present derivation

The fourth and final step of the derivation involves only the mechanics of calculus. The basic assumptions and the essential physical ideas (16) and (17) behind the wave slope distribution gave rise to (18), and now by differentiation of (18) with respect to ξ and to η, we have:

$$\phi'(\xi)\phi(\eta) = \frac{\xi}{(\xi^2+\eta^2)^{1/2}}\,\phi'((\xi^2+\eta^2)^{1/2})\phi(0) \qquad (21)$$

$$\phi(\xi)\phi'(\eta) = \frac{\eta}{(\xi^2+\eta^2)^{1/2}}\,\phi'((\xi^2+\eta^2)^{1/2}\ \phi(0) \qquad (22)$$

whence

$$\eta\phi'(\xi)\phi(\eta) = \xi\phi(\xi)\phi'(\eta)$$

or

$$\frac{\phi'(\xi)}{\xi\phi(\xi)} = \frac{\phi'(\eta)}{\eta\phi(\eta)} \quad . \qquad (23)$$

Since ξ and η are independent slope variables, this equality for arbitrary ξ and η requires each side to be of some arbitrary fixed value, say λ which we can choose to be -1 by the maximum property of the scatter diagram (a) of Fig. 12.54. Then:

$$\phi'(\xi) = -\xi\eta(\xi) \qquad (24)$$

and:

$$\phi'(\eta) = -\eta\phi(\eta) \quad .$$

In either case, we find:

$$\phi(\xi) = a'e^{-(1/2)\xi^2}$$
$$\phi(\eta) = b'e^{-(1/2)\eta^2} \qquad (25)$$

where a',b' are arbitrary constants. From (17):

$$\Phi(\xi,\eta) = a'b'\ e^{-(1/2)(\xi^2+\eta^2)}$$

and by definition of Φ:

$$\int_{-\infty}^{\infty}\int_{-\infty}^{\infty}\Phi(\xi,\eta)d\zeta_x d\zeta_y = 1$$

we find:

$$a'b' = \frac{1}{2\pi\sigma_u\sigma_c} \quad ,$$

so that:

$$\boxed{\Phi(\zeta_x,\zeta_y) = \frac{1}{2\pi\sigma_u\sigma_c}\ e^{-\frac{1}{2}\left[\left(\frac{\zeta_x}{\sigma_u}\right)^2+\left(\frac{\xi_y}{\sigma_c}\right)^2\right]}} \qquad (26)$$

It may be well to summarize the basic assumptions leading to (26). (i) the scatter diagram in (a) of Fig. 12.54 can be normalized and symmetrized by adopting the coordinates ξ,η as in (24) and (25) of Sec. 12.5, and the density of points is a maximum at the origin. (ii) The wave slope components ξ,η are independent (cf. (17)). The rest of the derivation, granting calculus operations possible, follows automatically. Therefore except for the symmetry assumption the basic assumptions leading to (26) are identical in kind to those leading to (12).

Observe, that if $\sigma_u = \sigma_c$, then since $\zeta_x^2 + \zeta_y^2 = \tan^2 \phi$, for ϕ in the context of Fig. 12.29, we obtain from (26) the probability distribution:

$$p(\tan \phi) = \frac{1}{2\pi\sigma^2} e^{-\left(\frac{\tan^2\phi}{2\sigma^2}\right)}, \qquad (27)$$

corresponding to (13) of Sec. 12.5. Furthermore, (26), as it stands, is the gaussian part of Cox and Munk's probability distribution for $p(\zeta_x,\zeta_y)$ given in (26) of Sec. 12.5.

Observe, finally, that the functional equation (18) which governs ϕ is the mathematical heart of the present derivation: all the physical assumptions were chosen so as to lead to (18) and all the essential mathematical deductions led from (18). Mathematical readers will note that the functional equation (18) is to the wave slope distribution, as the semigroup property is to the beam transmittance function (cf. (6) of Sec. 3.10 and also (3) of Sec. 3.11). Furthermore, the basic mathematical arguments leading to (12) and (26) are applicable to a wide range of physical phenomena beyond the present context (cf., e.g., [158]).

An alternate derivation of the slope distribution $p(\zeta_x,\zeta_y)$ which starts with the assumption that the sea surface is a sum of sine curves, is given for the one-dimensional case ($\zeta_y = 0$) by Cox and Munk in part III of [55]. This dervation leads to a one-dimensional Gram-Charlier representation of the form (26) of Sec. 12.5 (with $\eta = 0$) by considering a large finite number of superimposed sine waves. An interesting result of the derivation is some direct evidence for the existence of *continuous* wave spectra for ocean waves.

The Wavelength Distribution

We now return to the setting of Fig. 12.53 and reexamine the waves passing the wave pole. We shall use the notion of apparent wavelengths depicted in Fig. 12.51, and adduce a simple argument leading to a probability distribution of wavelengths and then go on to deduce a gamma type of wave spectrum ((16) of Sec. 12.8) for the temporal frequency σ. We shall initially assume that the waves are all traveling back and forth in a narrow band $\Delta\theta$ of directions about a given direction (shown by the arrows in Fig. 12.53).

By repeating the argument carried out in the case of wave slopes and leading to (26), or repeating the argument leading to (12), we can show that the relative number n_λ/n_o of occurrence of waves of wavelength λ passing the wave pole *in any direction* in the $\Delta\theta$ band is:

$$\frac{n_\lambda}{n_o} = e^{-\frac{\lambda^2}{2m}} \quad .$$

where we have assumed $\sigma_{\dot{u}}^2 = \sigma_{\dot{c}}^2 = m$ (now the mean square wavelength) and where n_o is the number of waves of average wavelength passing the pole. This representation is deliberately chosen to be similar to (13) of Sec. 12.5 so as to point up the basic similarity between the present derivation and that of (17) of Sec. 12.5. Indeed, we may use Fig. 12.29 and (a) of Fig. 12.54 to represent the distribution of wavelengths of waves traveling in various directions past the wave pole. The distances from the origin to the crosses in (a) of Fig. 12.54 are now values of λ. From this mode of representation, we see that the relative number $d\hat{n}_\lambda$ of waves of wavelength λ occurring in the $\Delta\theta$ sector of the ring of radius λ and thickness $d\lambda$ is:

$$d\hat{n}_\lambda = (\Delta\theta\lambda)\,\frac{n_\lambda}{n_o}\,d\lambda = \Delta\theta C\lambda e^{-\frac{\lambda^2}{2m}}\,d\lambda \quad ,$$

where we choose C so that the total relative number of waves over the whole λ-plane is 1. Hence, analogously to (17) of Sec. 12.5, we have:

$$\boxed{\hat{n}_\lambda = 1 - e^{-\frac{1}{2}\frac{\lambda^2}{m}}} \quad . \tag{28}$$

The density distribution $d\hat{n}_\lambda/d\lambda$ as a function of λ is of particular interest at present. Writing "T_λ" for $d\hat{n}_\lambda/d\lambda$ we have:

$$\boxed{T_\lambda = \frac{\lambda}{m}\,e^{-\frac{1}{2}\frac{\lambda^2}{m}}} \quad . \tag{29}$$

As it stands, T_λ is simple a *Rayleigh distribution* in the wavelength parameter λ. This Rayleigh distribution occurs often in statistical physical situations where some parameter (such as λ) varies randomly over the interval $(0,\infty)$ rather than over $(-\infty,\infty)$. Indeed, a Rayleigh distribution may be thought of as the distribution of the *lengths* (i.e., scalar components) of *vectors* (i.e., directional entities) which are suitably randomly distributed over some domain. It is now clear that we can relax the condition of a narrow band of directions and redo the derivation with $\Delta\theta = 2\pi$, if desired. We will arrive once again at (29).

The Bretschneider Spectrum

We can convert (29) into a gamma type spectrum of the form given in (16) of Sec. 12.8, as follows. We assume that there is some constant, say β, such that:

$$\lambda = \beta\tau^2 \tag{30}$$

for apparent wavelengths and periods. For example, if we have the purely periodic sinusoidal waves of the classical wave theory, then, according to (2) of Sec. 12.8, $\beta = g/2\pi$. If the waves are distributed according to the Neumann spectrum, then by (3) of Sec. 12.8, $\beta = (2/3)(g/2\pi)$. In general then, β depends on the distribution in question. From (30) we have:

$$\lambda = \beta(2\pi/\sigma)^2 = 4\pi^2\beta\sigma^{-2} \tag{31}$$

so that:

$$d\lambda = -\ 8\pi^2\beta\sigma^{-3}\ d\sigma \quad . \tag{32}$$

Writing:

$$\text{"}T_\sigma\text{"} \quad \text{for} \quad T_\lambda \left|\frac{d\lambda}{d\sigma}\right| \tag{33}$$

we arrive at:

$$T_\sigma = \frac{4\pi^2\beta\sigma^{-2}}{m}\ e^{-\frac{1}{2m}\ [4\pi^2\beta]^2\sigma^{-4}}\ (8\pi^2\beta\sigma^{-3})\ d\sigma\ , \tag{34}$$

that is:

$$\boxed{T_\sigma = a\sigma^{-5}\ e^{-\left(\frac{b}{\sigma U_a}\right)^4}} \tag{35}$$

where we have written:

$$\text{"a"} \quad \text{for} \quad \frac{32\pi^4\beta^2}{m} \tag{36}$$

$$\text{"b"} \quad \text{for} \quad \left[\frac{8\pi^4\beta^2}{m}\right]^{1/4} U_a \quad . \tag{37}$$

Hence in the context of (16) of Sec. 12.8, $p = 5$ and $q = 4$, and we have deduced the form of Bretschneider's spectrum (13) of Sec. 12.8. (Note that T_σ in (35) must be renormalized to be used for the evaluations discussed in Sec. 12.4.) In addition to the empirical evidence for T_σ referred to in the discussions of (13) of Sec. 12.8, we now have some theoretical evidence in its favor in the form of (35). But (35) must

still be viewed in the light of the critique of (21) and (22) of Sec. 12.8, and also as a consequence of the assumptions that led to it.

The Wave Height Distribution

In a manner exactly analogous to that just completed, we can show (by replacing "λ" everywhere by "H") that, corresponding to (29), we have:

$$T_H = \frac{H}{m} e^{-\frac{H^2}{2m}} \quad . \tag{38}$$

T_H is the probability distribution for wave height H(= 2X (amplitude)) so that T_H and T_λ are both Rayleigh distributions. The quantity m is now the root mean square wave height. A derivation of (38) was first given by Longuet-Higgins, and various consequences drawn from it are available in [164]. In view of (29), these consequences for H (or amplitude a) can then be applied, *mutatis mutandis*, to the wavelengths λ.

A study of the derivation of (38) and the properties of vector wave numbers in Fig. 12.16 seems to give the key to the answer to the question of why wave numbers will not work in the derivation of a formula like (29): the overall *resultant* of two wave forms is governed not by $\mathbf{k} = (1/2)\cdot(\mathbf{k}_1+\mathbf{k}_2)$ but by $\Delta k = (1/2)(\mathbf{k}_1-\mathbf{k}_2)$. (See the discussion of (99) of Sec. 12.3.) However, Rayleigh distributions are derived from superposition formulas of the type $(1/n)(\mathbf{k} +\ldots +\mathbf{k}_n)$. This leaves the reciprocal λ of $k/2\pi$ as the only remaining possible simple parameter associated with wavelengths. The fact that the empirically verified formula (35) follows from (29) seems to bear out that λ (rather than $\mathbf{k}$) is the appropriate variable to use in the deduction of the gaussian type distribution (27).

Models of Wind-Generated Spectra

We turn now to review some relatively recent and advanced theories of wind-generated waves. These theories go deeper into the physical wave generation processes than those reviewed above, by incorporating the hydrodynamic equations directly into the statistical treatment and by using harmonic analysis techniques of representing the dynamic air-water surface and the wind blowing over it. Despite the formidable analytical tools needed for a full unfolding of the description of the wave generation process, it is still possible to list and describe in simple terms the principal physical effects of the wind which have been considered pertinent to the generation process. These are as follows:

(i) *The Kelvin-Helmholtz Model.* In this model the air flows smoothly with horizontal streamlines over the flat water surface at speed U_a with the body of water possibly in its own smooth translatory motion of speed U_w. Then, as noted in (89) of Sec. 12.3, when $|U_a - U_w|$ is great enough, the tiny irregularities usually found on the real air-water surface, as predicted, grow exponentially with time. The active physical mechanism in this model is not immediately clear since the instability is simply the manifestation of the two roots of a quadratic equation becoming complex as $|U_a - U_w|$ becomes sufficiently large. However, Bernoulli effects, which are permissible in the simple physical setting of the Kelvin-Helmholtz model, may be the pertinent operative effects in this model.

(ii) *The Sheltering Model.* When one places his hand out the window of a moving vehicle and holds it against the force of the wind, one notes that the normal force on the palm increases systematically as the palm is turned full into the wind. If one replaces the palm with a plane surface and lets the stream of air of speed U_a push against it at an angle θ from the plane, then the pressure normal to the surface is known (Art. 77, [149]) to vary as:

$$\frac{\sin \theta}{\left(\frac{4}{\pi}\right) + \sin \theta} ,$$

with θ, and as:

$$\rho_a U_a^2$$

with wind speed U_a and air density ρ_a. If the plane surface is instead a facet of water surface, then the normal wind force on the facet is very nearly of the form:

$$s\rho_a U_a^2 \frac{\partial \zeta}{\partial x} \qquad (39)$$

where $\partial\zeta/\partial x$ now approximates $\tan \theta$, which for small θ in turn approximates $\sin \theta$ (and hence is proportional to $\sin \theta/[(4/\pi) + \sin \theta]$). The belief that the term (39) constituted the principal wave generating effect of the wind was called the *sheltering hypothesis* by Jeffreys [121] and was used as the starting point for his sheltering model. What is "sheltered" in this theory are the leeward sides of waves on a wind-blown sea. The normal force (39) acts on the windward side of the waves and because the leeward side has only an ineffective turbulent pressure on it, (39) acts as a driving force to push into and thereby feed kinetic energy to the waves. The horizontal driving force is $s\rho_a U_a^2 (\partial\zeta/\partial x)^2$, and if U_a is sufficiently great, instability will arise as in the Kelvin-Helmholtz model. The *sheltering coefficient* s forms a serious obstacle to the use of the sheltering model as it must be determined empirically, a determination which to this day (1966) is quite beyond available techniques.

(iii) *The Laminar Flow Model.* Wuest [324] in 1949 and Lock [161] in 1954 took into account the viscosity of the air

which allows a boundary layer to be formed. The wind can thereby impart a forward dragging force on the water surface. If a small, vertical, oscillatory motion in the lamina of air is introduced, say by the irregularities in the air-water surface, and if the lamina speed is great enough, then instabilities will arise as in the Kelvin-Helmholtz model and waves will be generated.

(iv) *The Stochastic Pressure Model.* In addition to the horizontal push and viscous drag of wind on already formed waves, the sudden downward gusts and sudden partial vacuums over an otherwise still water surface can effectively act to set the water mass into motion. In 1954 Eckart [86] combined the equations of hydrodynamics with the techniques of harmonic analysis to form a stochastic model of wind pressures acting in a storm area over a part of the sea. The model goes far toward the description of waves by this pressure mechanism, but on comparison with observed wind pressures, it turns out that the theory requires about ten times as much wind pressure as observed in the actual storms to generate the actual observed wave heights. Despite this inability of the stochastic wind pressure model to account fully for the observed wind-generated waves, the pioneering use of harmonic analysis techniques set the stage for the construction of later models.

(v) *The Stochastic Resonance Model.* A direct outgrowth of Eckart's model is that proposed in 1957 by Phillips [197]. The central feature of this model is the spatial Fourier analysis of air pressures over the air-water surface with an eye toward the *selective resonance* that one or more of these components may set up in the free water surface. One practical feature of this model is the derivation of the form of the time-dependent resolved directional energy spectrum $E(\mathbf{k},t)$ (cf. (75) of Sec. 12.4; see also (61) and (77) of Sec. 12.4). (See also [195], [196].)

(vi) *The Shear Flow Model.* This model, proposed in 1957 by Miles [179], builds on both the Kelvin-Helmholtz instability model and the Jeffreys sheltering model and goes beyond the latter in being able to calculate an equivalent of the sheltering coefficient. The actual mechanism of energy transfer from the air to the water is through an inviscid shear flow in the air layer above the water; the transfer proceeds at a rate proportional to the wind-profile curvature, $d^2U_a(y)/dy^2$ at the elevation where $U_a = c$ (c is the celerity of the water waves).

This model appears to yield some results in quantitative agreement with experimental data but is not wholly confirmed at present (1971).

The preceding six models of wave-generating wind-processes are all but parts of a currently incomplete and vastly complex puzzle as to how wind generates water waves in air-water surfaces. The final answer is certain to combine each of the preceding models as an integral part with varying

weights of importance, with perhaps a mechanism or two so far neglected. Such a synthesis has yet to be made.*

Spectral Transport Theory

The six models of wave generation processes reviewed above form but a small part of the entire problem of describing the evolution of waves on the air-water surface. Once the waves have been generated by either wind or other agents, their interactions one with the other, and their decay in time and space must be taken into account. Thus, quite analogously to photon (radiative) transport processes, we can formulate the general spectral transport process in terms of a general nonlinear integrodifferential equation for the directional energy spectrum $E(\mathbf{x},t,\mathbf{k})$: If D/Dt is the Lagrangian derivative operator ((5) of Sec. 3.15), then:

$$\frac{DE(\mathbf{x},t,\mathbf{k})}{Dt} = -\alpha(\mathbf{x},t,\mathbf{k})E(\mathbf{x},t,\mathbf{k}) + \int_{E_2} \mathcal{P}(E,E',\mathbf{x},t,\mathbf{k},\mathbf{k}')dV(\mathbf{k}') + E^{\circ}(\mathbf{x},t,\mathbf{k}) \tag{40}$$

where in the integrand we have written

"E' " for $E(\mathbf{x},t,\mathbf{k}')$

and

" E " for $E(\mathbf{x},t,\mathbf{k})$

and where $\mathcal{P}$ is the *interaction functional* describing the net rate of increase of $E(\mathbf{x},t,\mathbf{k})$ as a result of interactions of waves described by $E(\mathbf{x},t,\mathbf{k}')$, $\mathbf{k} \neq \mathbf{k}'$. The first term on the right is a decay term and the last term $E^{\circ}(\mathbf{x},t,\mathbf{k})$ describes the source term for E, and may be found by a suitable synthesis of any or all of the wind generation models discussed above. The central problem in current spectral transport theory is the exact delineation of the form of the interaction functional $\mathcal{P}$. The basic similarity of (40) to the equation of transfer, or the nonlinear Boltzmann equation of gas dynamics, or still more generally, its kinship with the Boltzmann equation of general stochastic theory [48] should lead, with the possible help of the nonlinear hydrodynamic equations (15), (16) of Sec. 12.3, and turbulence theory [10] to some specific representations of $\mathcal{P}$. Once this is done, solution procedures of (40) of various kinds can be studied ranging from iterative and perturbation procedures to closed forms

---

*For the status of this problem at the time of publication, see T. P. Barnett, and K. E. Kenyon, "Recent Advances in the Study of Wind Waves," Rep. Prog. Phys., 38, 667 (1976).

in the simpler cases of $\mathcal{P}$. At present very little is known about the form of $\mathcal{P}$. Some approximate perturbation techniques by Hasselmann [105] have yielded low order approximations to $\mathcal{P}$, but otherwise our knowledge of $\mathcal{P}$ is sparse. See also [106], [297], and [268].

As an indication of the use of $E(\mathbf{x},t,\mathbf{k})$ once (40) has been solved, we recall, e.g., the definition of $F(\sigma,\phi)$ in (107) of Sec. 12.4. If we then write:

$$\text{"}F(\mathbf{x},t,\sigma,\phi)\text{"} \quad \text{for} \quad E(\mathbf{x},t;\mathbf{k})\,\frac{\partial(u,v)}{\partial(\sigma,\phi)} \tag{41}$$

where now $\mathbf{k} = (u,v)$, and also write:

$$\text{"}T_\sigma(\mathbf{x},t)\text{"} \quad \text{for} \quad \int_0^{2\pi} F(\mathbf{x},t,\sigma,\phi)\,d\phi \quad , \tag{42}$$

we would then have the general space-variable, time-dependent version of T_σ in (110) of Sec. 12.4, and we would be able to have an overview of the Neumann, Bretschneider and other gamma-type spectra (16) of Sec. 12.8 and thereby be able to see how they fit into the general scheme of things. Furthermore, corresponding to (116)-(119) of Sec. 12.4, we would, for example, have for each point $\mathbf{x}$ and time t on the air-water surface:

$$m_{oo}(\mathbf{x},t) = \int_0^\infty T_\sigma(\mathbf{x},t)\,d\sigma \qquad \text{(mean square wave elevation)} \tag{43}$$

$$m_{2o}(\mathbf{x},t) = \frac{1}{g^2}\int_0^\infty\int_0^{2\pi} F(\mathbf{x},t,\sigma,\phi)\sigma^4\cos^2\phi\;d\phi\;d\sigma \tag{44}$$

(mean square wave slope along x axis)

$$m_{o2}(\mathbf{x},t) = \frac{1}{g^2}\int_0^\infty\int_0^{2\pi} F(\mathbf{x},t,\sigma,\phi)\sigma^4\sin^2\phi\;d\phi\;d\sigma \tag{45}$$

(mean square wave slope along y axis)

$$m_{11}(\mathbf{x},t) = \frac{1}{g^2}\int_0^\infty\int_0^{2\pi} F(\mathbf{x},t,\sigma,\phi)\sigma^4\sin\phi\cos\phi\;d\phi\;d\phi \;. \tag{46}$$

These moments, in turn, would supply the basic input data needed in the theory of the calculation of the average reflection and transmission properties of the dynamic air-water surface with respect to incident radiant flux. We shall now turn to the construction of such a theory.

<< Table of Contents **<< Title Page >>** **Next Page >>**